Title

Conceptualizing Biogeochemical Reactions With an Ohm's Law Analogy

Journal

Journal of Advances in Modeling Earth Systems, 13(10)

ISSN

1942-2466

Authors

Tang, Jinyun
Riley, William J
Marschmann, Gianna L
et al.

Publication Date

2021-10-01

DOI

10.1029/2021ms002469

JAMES | Journal of Advances in Modeling Earth Systems

RESEARCH ARTICLE
10.1029/2021MS002469

Key Points:

- Ohm's law is proposed to formulate biogeochemical reactions
- Ohm's law successfully represents multiple-nutrient-colimited growth
- Ohm's law may help improve and unify biogeochemical models

Supporting Information:

Supporting Information may be found in the online version of this article.

Correspondence to:

J. Tang,
jinyuntang@lbl.gov

Citation:

Tang, J., Riley, W. J., Marschmann, G. L., & Brodie, E. L. (2021). Conceptualizing biogeochemical reactions with an Ohm's law analogy. *Journal of Advances in Modeling Earth Systems*, *13*, e2021MS002469. https://doi.org/10.1029/2021MS002469

Received 11 JAN 2021
Accepted 28 SEP 2021

Author Contributions:

Conceptualization: Jinyun Tang
Formal analysis: Jinyun Tang
Funding acquisition: Jinyun Tang, William J. Riley, Eoin L. Brodie
Investigation: Jinyun Tang
Writing – original draft: Jinyun Tang
Writing – review & editing: William J. Riley, Gianna L. Marschmann, Eoin L. Brodie

Conceptualizing Biogeochemical Reactions With an Ohm's Law Analogy

Jinyun Tang[1], William J. Riley[1], Gianna L. Marschmann[1], and Eoin L. Brodie[1]

[1]Earth and Environmental Sciences Area, Lawrence Berkeley National Laboratory, Berkeley, CA, USA

Abstract In studying problems like plant-soil-microbe interactions in environmental biogeochemistry and ecology, one usually has to quantify and model how substrates control the growth of, and interaction among, biological organisms (and abiotic factors, e.g., adsorptive mineral soil surfaces). To address these substrate-consumer relationships, many substrate kinetics and growth rules have been developed, including the famous Monod kinetics for single-substrate-based growth and Liebig's law of the minimum for multiple-nutrient-colimited growth. However, the mechanistic basis that leads to these various concepts and mathematical formulations and the implications of their parameters are often quite uncertain. Here, we show that an analogy based on Ohm's law in electric circuit theory is able to unify many of these different concepts and mathematical formulations. In this Ohm's law analogy, a resistor is defined by a combination of consumers' and substrates' kinetic traits. In particular, the resistance is equal to the mean first passage time that has been used to derive the Michaelis-Menten kinetics under substrate replete conditions for a single substrate as well as the predation rate of individual organisms. We further show that this analogy leads to important insights on various biogeochemical problems, such as (a) multiple-nutrient-colimited biological growth, (b) denitrification, (c) fermentation under aerobic conditions, (d) metabolic temperature sensitivity, and (e) the legitimacy of Monod kinetics for describing bacterial growth. We expect that our approach will help both modelers and nonmodelers to better understand and formulate hypotheses when studying certain aspects of environmental biogeochemistry and ecology.

Plain Language Summary Currently, scientists often use ad hoc or empirical approaches to conceptualize and formulate biogeochemical processes encountered in environmental sciences. Here, we propose that many biogeochemical processes can be coherently conceptualized and formulated using an analogy based on Ohm's law, a mathematical theory that is widely used to model electric circuits, and the land-atmosphere exchange of water and energy. We show that this Ohm's law analogy is able to explain observations such as why microbial growth often follows Monod kinetics, how fermentation can sometimes dominate aerobic respiration when glucose is plentiful, and how plants and microbes grow under multiple-nutrient-colimitation. Since this Ohm's law analogy unifies the mathematical foundation of biogeophysics and biogeochemistry, we believe that it can potentially lead to more robust land ecosystem models for projecting the climate change.

1. Introduction

In earth system modeling, biogeochemistry strongly affects mass and energy exchanges between ecosystems and the physical climate system (Heinze et al., 2019). Morphologically, biogeochemistry has three pillars: biology, geophysics, and chemistry. In the context of mathematical modeling, geophysics and chemistry generally have much stronger theoretical foundations than biology (Brutsaert, 2005; Stumm & Morgan, 1996; Vallis, 2006), even though all three are macroscale responses that emerge from atomic interactions, which in an ideal (but impractical) scenario can be predicted by solving the Schrödinger equation of all atoms together (so that arguably they all are subtopics of physics; Feynman et al., 2011c).

In seeking a better understanding of ecological dynamics, for example, competition and symbiosis, mathematical formulations of the substrate-consumer relationship (e.g., the interactions between many microbes as consumers and their diverse substrates) are essential for theoretical modeling and interpreting empirical experiments, such as phytoplankton population dynamics (Tilman, 1982), plant-microbial competition of nutrients (Zhu et al., 2017), and microbial decomposition of organic matter (Tang & Riley, 2013b; Yu

et al., 2020). In the past, three approaches have been used to obtain such relationships. The first approach is by fitting empirical response functions to observational data (e.g., Monod, 1949). The second approach is based on an ad hoc heuristic conceptualization of the problem, for example, the logistic equation was derived by adding a quadratic term to dissipate the exponential growth of a population when Pierre-Francois Verhulst was helping his teacher Alphonse Quetelet to model human population dynamics (Cramer, 2002). The third approach is based on systematic applications of some theory, such as the law of mass action (Atkins et al., 2016), statistical mechanics (Ma, 1985), or renewal theory (Doob, 1948). Notably, Michaelis-Menten kinetics (and some of its extensions) can be derived by applying any of these theories (see reviews in Kooijman, 1998; Swenson & Stadie, 2019; Tang & Riley, 2013b, 2017), with the renewal theory even being able to show that Michaelis-Menten kinetics is the statistical mean of the stochastic description of a single-enzyme molecule processing the substrate molecules (English et al., 2006; Reuveni et al., 2014).

Compared to the empirically based and ad hoc approaches, which generally provide limited understanding of the processes implied by the parameters, theory-based approaches have the advantage of linking various related, albeit fragmented, knowledge (that is abstracted from a much wider range of observations compared to the limited observational data used by empirically based approaches), thereby enabling a deeper understanding of the processes and systems of interest. For instance, when the law of mass action is employed to derive the Michaelis-Menten kinetics, using related theory of chemical reaction rates (e.g., Smoluchowski's diffusion model of chemical reaction, von Smoluchowski, 1917), Tang and Riley (2019a) were able to upscale the microbially enabled reactions from one permease to a single bacteria cell and then to a representative soil volume (~O(1 cm^3)) and used the results to explain why substrate affinity parameters are observed to be highly variable in soil. Additionally, the theory-based approach has been used to derive the temperature response function of microbial activity (Ghosh & Dill, 2010) and to explain why Michaelis-Menten kinetics are more appropriate for microbial uptake of small molecules, while reverse Michaelis-Menten kinetics are more appropriate for enzymatic degradation of organic polymer particles (Tang & Riley, 2019b).

In this study, we first introduce an analogy that uses the Ohm's law from electric circuit theory to interpret substrate-consumer relationships. Similar analogies have been widely used by land models to represent the gradient-driven land-atmosphere exchanges of water, gases, and energy (e.g., Lawrence et al., 2019; Riley et al., 2011; Shuttleworth & Wallace, 1985; Wu et al., 2009; so that in a certain sense, Ohm's law is unifying all three aspects of biogeochemistry into physics). We then exploit this analogy to explain several interesting biogeochemical phenomena that are observed in different contexts. We conclude the paper with recommendations of other potential applications of this analogy.

Although the example problems below are solved with the Ohm's law analogy, we note that they can all be solved using the more accurate equilibrium chemistry approximation (ECA) kinetics (Tang & Riley, 2013b) or the synthesizing unit plus ECA (SUPECA) kinetics (Tang & Riley, 2017). However, the Ohm's law analogy proposed here is more intuitive and can provide an alternative to the ECA and SUPECA kinetics in formulating biogeochemical models.

2. Methods

2.1. A Brief Review of Ohm's Law and Circuit Theory

We below briefly review Ohm's law and the theory of series and parallel resistor circuits. More detailed descriptions of circuit theory can be found in Feynman et al. (2011b).

Ohm's law describes the relationship between voltage (V), electric current (I), and resistance (r) as

$$I = \frac{V}{r} \tag{1}$$

To simplify the presentation, we henceforth assume that all variables are properly defined as in the international system of units.

For a series concatenation of resistors r_j, application of Ohm's law yields

$$I = \frac{V}{\sum_j r_j} \tag{2}$$

For a parallel concatenation of resistors r_j, application of Ohm's law leads to

$$I = V\left(\Sigma_j \frac{1}{r_j}\right) \tag{3}$$

and the electric current through each resistor is

$$I_j = \frac{V}{r_j} \tag{4}$$

From Equations 3 and 4, we can further derive

$$\frac{I_j}{I} = \frac{1}{1+\left(\Sigma_{l\neq j}\frac{r_j}{r_l}\right)} \tag{5}$$

which states that when all other resistors are fixed, the fraction of current through r_j increases with decreasing r_j. We will see later that this inference is very useful to explain shifts in metabolic pathways in biological organisms.

As another analogy, Ohm's law has also been used to represent soil evaporation (Bonan, 2019; Tang & Riley, 2013a), where voltage is calculated as the difference between atmospheric and soil water vapor concentrations, resistance is the sum of atmospheric and soil resistance, and current is the evaporation flux.

2.2. Michaelis-Menten Kinetics Interpreted With Ohm's Law

Michaelis-Menten kinetics represent the single-enzyme-catalyzed single-substrate reaction velocity v as

$$v = \frac{v_{\max} ES}{K+S} \tag{6}$$

where, in the original application by Michaelis and Menten (1913), v_{max} is the maximum specific catalytic rate enabled by the enzyme and E, S, and K are enzyme concentration, substrate concentration, and half saturation coefficient, respectively. We note that, for enzymes, K also includes contributions from the dissociation process (e.g., Briggs & Haldane, 1925).

By defining $k_f = v_{\max}/K$, Equation 6 can be rewritten as

$$v = \frac{E}{\left(1/v_{\max}\right)+\left(K/v_{\max}S\right)} = \frac{E}{\left(1/v_{\max}\right)+\left(1/k_f S\right)} \tag{7}$$

We then note that Equations 1 and 7 are mathematically of the same form. Therefore, for Michaelis-Menten kinetics, if we apply the Ohm's law analogy by regarding E as voltage and v as current, the corresponding resistance is

$$r = \frac{1}{v_{max}} + \frac{1}{k_f S} = r_E + r_S \tag{8}$$

where r_E represents the resistance as an intrinsic property (i.e., a kinetic trait) of the enzyme, and r_S represents the resistance introduced by the effective substrate delivery rate toward the enzyme (i.e., a kinetic trait of the substrate in the working environment of the enzyme). Further, r_E and r_S are of the unit of time, where (in the renewal theory applied to enzyme-substrate interactions, e.g., Kooijman, 1998) r_E is the mean time for the enzyme to convert the enzyme-bound substrate molecules into product molecules and r_S is the mean time for the substrate molecules to approach the enzyme molecule and form enzyme-substrate complexes. Therefore, r is the mean first passage time of the stochastic single-enzyme degradation of the substrate molecule (e.g., Kooijman, 1998; Ninio, 1987; Qian, 2008). In particular, in many reactions, k_f is approximately proportional to the substrate diffusivity (Alberty & Hammes, 1958; Chou & Jiang, 1974), such that $k_f S$ is the diffusive substrate flux sensed by enzyme molecules. We then observe that r_S increases with the decrease of diffusive substrate flux, which can result from lower substrate concentration or lower diffusivity (due to tortuosity, adsorption, or lower moisture in porous media like soil). In Tang and Riley (2019a), the relationship between r_S and diffusivity has enabled a way to parameterize how soil moisture affects microbial substrate uptake, which probably can also be used to parameterize how soil moisture affects plant root uptake of macronutrients.

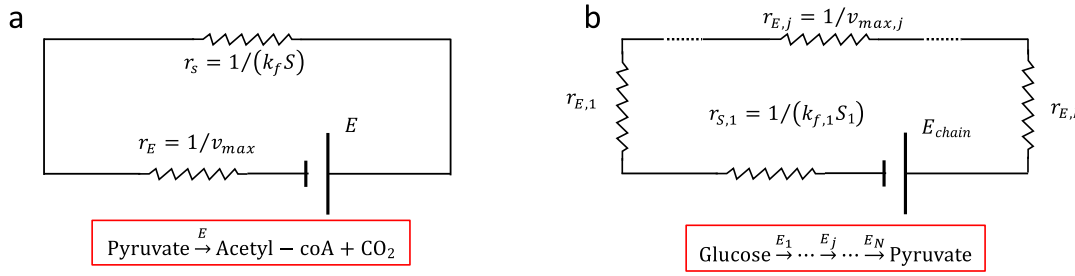

Figure 1. (a) Circuit schema for the Michaelis-Menten kinetics, with the example (in red box) depicting the conversion of pyruvate into acetyl-coA and CO_2 by the enzyme complex pyruvate dehydrogenase complex; (b) Series resistor-based schema for an enzyme chain and its reaction on substrate S_1, where dotted lines indicate multiple resistors $r_{E,j}$ concatenated in series. Symbols are explained in the main text. The example for (b) depicts the metabolic pathway of glycolysis.

Alternatively, for high-enzyme concentration systems (such as the hydrolysis of cellulose, Kari et al., 2017; Tang & Riley, 2019b), where the reverse Michaelis-Menten kinetics better describe the dynamics, we have

$$v = \frac{S}{\left(1/v_{\max}\right) + \left(K/v_{\max}E\right)} = \frac{S}{\left(1/v_{\max}\right) + \left(1/k_f E\right)} \tag{9}$$

where substrate S instead plays the role of voltage, and $1/\left(k_f E\right)$ defines the resistance due to the effective deployment rate of enzyme E to the substrate. Comparing Equations 8 and 9, we see that the roles of substrate and enzyme in the Ohm's law analogy are context dependent.

That the resistance r in Equation 8 is of the unit time has also motivated some researchers to apply the time-budget idea to derive predator-prey relationships (e.g., Holling, 1959; Murdoch, 1973), where r_E is referred as the mean time a predator spends on handling its prey, and r_S is the mean time for a predator to encounter its prey. Further, McAdams and Shapiro (1995) noticed that the circuit analogy can be used to interpret and model genetic networks. However, few studies have pointed out the linkage between the time-budget analysis and Ohm's law, except, based on a suggestion by Thomsen et al. (1994), Almeida et al. (1997) made an analogy of the membrane electron transport chain to an electric circuit, and successfully used it to model denitrification. Later, Murkin (2015) suggested that the Ohm's law may be used to help students better understand enzyme kinetics in teaching biochemistry. Recently, this method has been used by Domingo-Felez and Smets (2020) to build the Activated Sludge Model-Electron Competition (ASM-EC) model, which demonstrated the efficacy of this analogy in constructing robust biogeochemical models. Further, the molecular biology of membrane electron transport chains and redox reactions are quite similar to the working principles of chemical batteries (Frederiksen & Andresen, 2008; Schmidt-Rohr, 2018), thereby motivating us to explore more extensively the applicability of Ohm's law analogy below.

In the Ohm's law analogy, kinetic interactions between an enzyme and its substrate molecules can be summarized as the battery-resistor relationship shown in Figure 1a, where the battery potential is enzyme concentration E, and the battery's resistance is r_E, while the resistor (i.e., substrate) has resistance r_S. However, we note that this analogy is accurate only when the substrate is nonlimiting for the enzymes (i.e., when Michaelis-Menten kinetics are more appropriate, Tang & Riley, 2019b). For cases when substrate is limiting, the reverse Michaelis-Menten kinetics are more appropriate (Tang, 2015), and the roles of substrate and enzyme in the analogy are reversed (see Equation 9). We also note that the ECA kinetics are able to more accurately handle the wide range of substrate abundances with respect to enzymes (Tang, 2015). We next show how the Ohm's law analogy can help formulate biogeochemical kinetics for various situations.

3. Applications

3.1. Series Resistor Circuit-Based Formulation of Chain-Like Enzyme Reactions

Many metabolic pathways consist of a chain of reactions. Examples include the Calvin-cycle (in photosynthesis), membrane electron transport chain, glycolysis (Figure 1b), and citric acid cycle, and note that most of these reaction pathways involve cofactors (Madigan et al., 2009; Taiz & Zeiger, 2006). Nonetheless,

assuming that at each step the enzyme and its cofactor together form an integrated enzyme functional unit to process the substrate delivered from a prior step, and the whole chain of enzymatic reactions is in detailed balance (i.e., the whole chain is in steady state without overflow, Cao, 2011, an assumption that is often made in flux balance models, Orth et al., 2010), we can then use the series circuit analogy to calculate the overall enzyme kinetics in a straightforward manner. According to the schema for this configuration (Figure 1b), when the whole enzyme chain is taken as a catalysis unit, the abundance of enzyme at the first step represents the voltage of the battery, and the total resistance is

$$r_{\text{chain}} = \left(\sum_{j=1}^{N} r_{E,j}\right) + r_{S,1} = r_E + r_{S,1} \tag{10}$$

where $r_{E,j} = v_{\max,j}^{-1}$, such that the first right-hand side term is the total resistance represented by the maximum catalysis rate of the overall enzyme chain, and $r_{S,1} = \left(k_{f,1} S_1\right)^{-1}$ is the resistance due to the incoming substrate flux to the first enzyme in the chain. For the overall chain, the specific reaction rate for substrate processing is then

$$\frac{v_{\text{chain}}}{E_{\text{chain}}} = \frac{1}{r_{\text{chain}}} = \frac{\left(\sum_{j=1}^{N} v_{\max,j}^{-1}\right)^{-1} S_1}{\left(K_1 / v_{\max,1}\left(\sum_{j=1}^{N} v_{\max,j}^{-1}\right)\right) + S_1} \tag{11}$$

where $K_1 = v_{\max,1}/k_{f,1}$, and E_{chain} represents the enzyme functional unit (e.g., for the glycolysis metabolic pathway in Figure 1b, E_{chain} could be the amount of enzyme hexokinase E_1, assuming that all other enzymes are highly regulated in forming the chain of enzymes catalyzing related biogeochemical reactions). Equation 11 can be simplified as

$$\frac{v_{\text{chain}}}{E_{\text{chain}}} = \frac{v_{\max,\text{chain}} S_1}{K_{\text{chain}} + S_1} \tag{12}$$

with

$$v_{\max,\text{chain}} = \left(\sum_{j=1}^{N} v_{\max,j}^{-1}\right)^{-1} < \min_j \left\{v_{\max,j}\right\} \tag{13}$$

and

$$K_{\text{chain}} = \frac{K_1}{v_{\max,1}\left(\sum_{j=1}^{N} v_{\max,j}^{-1}\right)} = \frac{K_1}{1 + \sum_{j=2}^{N} v_{\max,1}/v_{\max,j}} \tag{14}$$

From Equation 11, we assert that an enzyme chain is equivalent to a functional enzyme unit with kinetic traits $v_{\max,\text{chain}}$ and K_{chain}. Moreover, from Equations 13 and 14, we infer that increasing the chain length decreases the overall reaction rate $v_{max,chain}$ (which is even slower than the slowest step $\min_j \left\{v_{\max,j}\right\}$) and the half saturation coefficient K_{chain} of the enzyme chain.

Several interesting inferences can be drawn from Equations 10–14 that will provide us with a better understanding of the trade-offs in metabolic pathways and their temperature sensitivity, both of which are essential for parameterizing biochemical models, such as microbial respiration (Alster et al., 2020), plant photosynthesis, and respiration (Medlyn et al., 2002; Slot & Kitajima, 2015). First, even though any chain-like metabolic pathway as a whole can be represented similarly with the Michaelis-Menten kinetics (e.g., Equation 12), there are trade-offs between power and bioenergetic assimilation efficiency for various metabolic pathways of different lengths, which can be understood as follows. The function of an energy producing metabolic pathway is to harvest energy from substrate molecules, we thence can compare an ATP producing metabolic pathway to a thermal engine which also extracts energy from substrate molecules (i.e., fuels). The second law of thermodynamics suggests that a thermal engine has higher thermodynamic efficiency when it runs slower (and the highest efficiency can be achieved only when the system is in thermodynamic equilibrium, i.e., not running at all, Salamon et al., 2001). Equation 13 suggests that a longer reaction chain slows down the overall transformation rate from a given substrate to its final product, and thus its application to electron transport chains leads us to assert that a longer chain will likely be thermodynamically more efficient (this argument echoes the Ladder theorem in finite time thermodynamics, Salamon et al., 2017). In contrast, shorter electron transport chains imply faster substrate use even though they are less efficient in extracting Gibbs free energy from the substrate. For instance, by using a different electron transporter for each electron transported through a shorter chain, fewer protons are pumped across the membrane and thus fewer ATPs can be produced (Chen & Strous, 2013), or by using fewer intermediate electron carriers

such that fewer protons are pumped across the membrane for each transferred electron (if generating one ATP uses a fixed number of protons as is often observed), the same redox reaction will be faster but less efficient (Aledo & del Valle, 2002; Chen & Strous, 2013). Therefore, the length of electron transport chains can characterize the trade-off between substrate use rate and the corresponding bioenergetic assimilation efficiency, an important selection factor for organisms during their evolution. Since the structural information of electron transport chain can be inferred by genomic analysis (Lane & Martin, 2010), this insight from the Ohm's law formulation can then serve to better guide model parameterization of plant and microbial substrate uptake and use. Additionally, we note that in microbial modeling, the metabolic cost for constructing and maintaining the chain of enzymes is usually considered separately as part of the respiration for maintenance or structural biomass growth and is thus not part of the calculation of a substrate's bioenergetic assimilation efficiency (Kooijman, 2009). Indeed, in one chemostat-based study, Chen et al. (2017) found that *Vibrionales* bypass respiratory complex III to consume part of the oxygen using a cytochrome bd terminal oxidase to speed up growth, but the bioenergetic efficiency was reduced from ~80% to ~32% because of the longer canonical respiratory chain. Similarly, observations indicate that the less efficient fermentation pathway with fewer involved enzymes is faster than the aerobic respiration pathway that involves many more enzymes (and is thus longer and more efficient in extracting Gibbs free energy from substrate molecules, Madigan et al., 2009). In Section 3.5, we use the parallel circuit analogy to explain why such bypassing of more efficient pathways will occur under substrate abundant conditions.

The second inference to be made is about the temperature sensitivity of parameters $v_{max,chain}$ and K_{chain}, two essential trait characteristics for biochemical modeling, whose mathematical parameterization (particularly for microbes) has been under intense debate (Allison et al., 2018; Davidson et al., 2012; Maggi et al., 2018).

In the simplest one-step case, $v_{max,chain}$ equals $v_{max,1}$, and K_{chain} equals K_1. According to transition state theory (e.g., Eyring, 1935), $v_{max,1}$ would have the following temperature dependence,

$$v_{\max,1} = v_{\max,1,ref} T \cdot \exp\left(-\frac{\Delta G_1}{RT}\right) \tag{15}$$

where $v_{max,1,ref}$ is some reference reaction rate, T is temperature, ΔG_1 (>0) is the Gibbs energy of activation, and R is the universal gas constant. Similarly, for a reaction pathway consisting of a chain of enzymes, each $v_{max,j}$ will have a temperature dependence similar to that in Equation 15, that is,

$$v_{\max,j} = v_{\max,j,ref} T \cdot \exp\left(-\frac{\Delta G_j}{RT}\right) \tag{16}$$

which when entered into Equation 13 leads to

$$v_{\max,\text{chain}} = \left[\sum_{j=1}^{N}\left(v_{\max,j,ref}^{-1} \exp\left(\frac{\Delta G_j - \Delta G_1}{RT}\right)\right)\right]^{-1} T \cdot \exp\left(-\frac{\Delta G_1}{RT}\right) \tag{17}$$

Therefore, if $\left(\Delta G_j - \Delta G_1\right)/\left(RT\right) \ll 1$, the temperature dependence of $v_{max,chain}$ will be approximately like that in Equation 15.

The temperature dependence of K_1 is determined by the temperature dependencies of $v_{max,1}$ and $k_{f,1}$. Inside the microbial cytoplasm and cell membrane (and also for whole microbial cells in most natural environments, and chloroplasts in mesophyll cells), $k_{f,1}$ is positively related to diffusivity (Madigan et al., 2009). Thus, according to the Stokes-Einstein equation of translational diffusivity ($D = \left(k_B T\right)/\left(6\pi\eta a\right)$, where k_B is the Boltzmann constant, η is the dynamic viscosity, and a is the radius of the spherical particle; Feynman et al., 2011a), $k_{f,1}$ can be approximated with a linear temperature dependence divided by the temperature sensitivity of the dynamic viscosity η (which is $exp\left(B/\left(T - T_{VF}\right)\right)$, where B and T_{VF} are empirical parameters, according to the semiempirical Vogel-Fulcher-Tamman-Hesse equation, Garcia-Colin et al., 1989). When the temperature dependence of $k_{f,1}$ is combined with the Eyring-type temperature dependence of $v_{max,1}$, one may infer that the temperature sensitivity of K_1 ($=v_{max,1}/k_{f,1}$) is of the Arrhenius type (because $exp\left(B/\left(T - T_{VF}\right)\right)$ of the dynamic viscosity η is very similar to the Arrhenius equation, and the linear temperature dependence of $k_{f,1}$ cancels out the linear part of the temperature dependence of $v_{max,1}$). Once again, if $\left(\Delta G_j - \Delta G_1\right)/\left(RT\right) \ll 1$, K_{chain} will have an Arrhenius-type temperature sensitivity as well.

When the above inferences are substituted to Equation 12, we can then infer the temperature dependence of v_{chain}. From chemical thermodynamics, the temperature dependence of v_{chain} depends on chemical kinetics (as characterized by the Michaelis-Menten term, i.e., $v_{max,chain}S_1/\left(K_{chain} + S_1\right)$ in this example) and thermodynamics (as a function of the Gibbs free energy) of the enzyme-catalyzed reaction (LaRowe et al., 2012). However, because enzymes are proteins, their conformational states are also temperature dependent (Murphy et al., 1990). Thermodynamically, the undenatured (aka catalytically active) fraction of an enzyme population of length n_x (as measured by the number of amino acid residues) can be described as (Murphy et al., 1990)

$$f_{ax} = \frac{1}{1 + exp\left(-\frac{n_x \Delta G_x}{RT}\right)} \tag{18}$$

where

$$\Delta G_x = \Delta H^* - T\Delta S^* + \Delta C_p\left[\left(T - T_H^*\right) - T\,ln\left(T/T_S^*\right)\right] \tag{19}$$

and

$$\Delta C_p = -46.0 + 30\left(1 - 1.54 n_x^{-0.268}\right)N_{CH,x} \tag{20}$$

with heat capacity ΔC_p defined as the energy required to reorganize the water molecules surrounding the protein (Ratkowsky et al., 2005). ΔC_p increases with the nonpolar accessible area of the molecule, as measured by $N_{CH,x}$, the average number of nonpolar hydrogen atoms per amino acid residue. ΔC_p also measures the hydrophobic contribution, with higher values implying higher hydrophobicity (and notice that greater $N_{CH,x}$ implies higher hydrophobicity). Other parameters include ΔS^* as the enthalpy change at T_S^* (the convergence temperature for entropy, i.e., the temperature at which the hydrophobic contributions to ΔS^* is zero) and ΔH^* as the enthalpy change at T_H^* (the convergence temperature for enthalpy, i.e., the temperature at which the hydrophobic contributions to ΔH^* is zero), among which ΔS^*, T_S^*, and T_H^* can be considered to be constant under environmental conditions, for example, Ratkowsky et al. (2005) took $T_H^* = 373.6$ K, $T_S^* = 385.2$ K, and $\Delta S^* = 18.1$ J K^{-1} (mol amino acid residue)$^{-1}$, respectively. Assuming ΔH^*, $N_{CH,x}$, and n_x can be obtained from proteomic data for each type of enzyme (e.g., Sawle & Ghosh, 2011), we can then calculate $f_{ax,j}$ for all enzymes involved in the chain. Therefore, putting together the kinetic, thermodynamic, and catalytically active enzyme fraction functions, we obtain

$$v_{chain} = \frac{v_{max,chain}S}{K_{chain} + S} F_T \prod_j f_{ax,j} \tag{21}$$

where the thermodynamic temperature dependence of the reaction is

$$F_T = 1 - exp\left(\frac{\Delta G_{reac}}{RT}\right) \tag{22}$$

with ΔG_{reac} (<0) being the Gibbs free energy of the overall reaction being catalyzed, which is defined by the chemical activity of initial substrates and final products for the overall chemical reaction carried out by the chain of enzymes (e.g., Jin & Bethke, 2007). In Equation 21, we have taken the conventional assumption that the transition state theory description of the overall chemical reaction rate (as carried out by the chain of enzymes) is independent from the conformation status of the enzymes (Dill et al., 2011; Sawle & Ghosh, 2011). This assumption combined with the concept that F_T is an intrinsic property of the overall chemical reaction then allows the total fraction of active enzymes to be factored out as $\prod_j f_{ax,j}$. (Note that $f_{ax,j}$ can be viewed as the probability for enzyme j to be in the conformed state, thus, by the theory of conditional probability, the probability for the whole enzyme chain to be in active status is $\prod_j f_{ax,j}$.)

Unless Equation 21 is applied to organisms capable of growing on alternative electron acceptors or donors and the system is undergoing fast transition in redox status (e.g., heterotrophic microbes in the fluctuating zone of soil water table, Zhang & Furman, 2021), F_T can be taken approximately as 1. Therefore, the temperature dependence of v_{chain} is dominated by the kinetic term (i.e., the Michaelis-Menten term) and the temperature-dependent fraction of active enzymes ($\prod_j f_{ax,j}$). The kinetic term increases with temperature (see Equation 16), while the fraction of active enzymes first increases, then decreases with temperature (Equations 18–20). The overall temperature sensitivity of the reaction chain will then be of the form predicted by the macromolecular rate theory (MMRT; with fine tuning from substrate availability through the

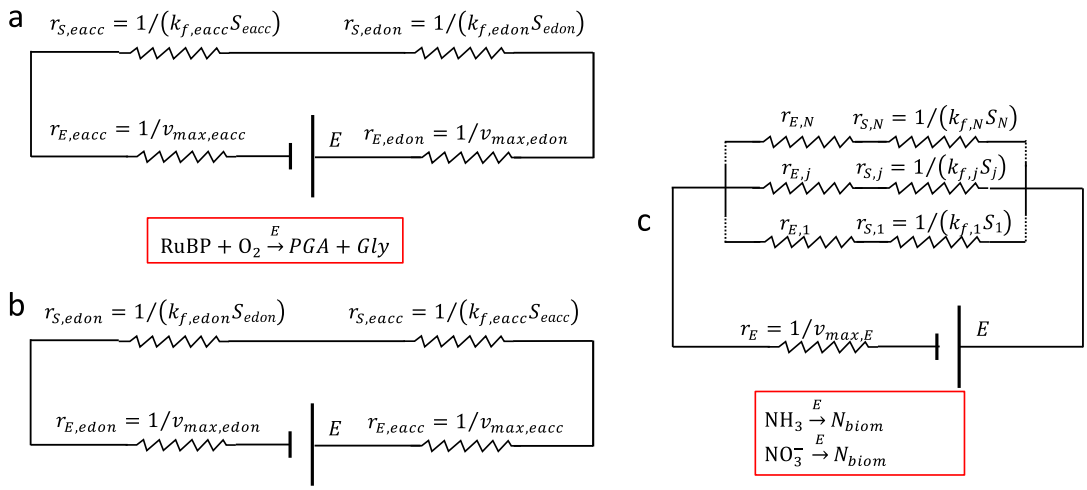

Figure 2. (a) Type-1 circuit schema for redox-type reactions where electron donor binds before the electron acceptor to the enzyme, with the example (in red box) depicting the binding of RuBP (ribulose 1,5-bisphosphate) and O_2 to Rubisco enzyme to produce PGA (3-phosphoglycerate) and Gly (glycine) in the oxygenation pathway of photosynthesis; (b) Type-2 circuit schema for redox-type reactions where electron acceptor binds before electron donor to the enzyme; (c) Circuit schema for parallel resistor-based representation of competitive enzymatic reactions, with an example of an organism (in the red box) building biomass from assimilating ammonia and nitrate as substitutable nitrogen sources. Type-1 and type-2 schema are equivalent and are not differentiated in the Ohm's law analogy based on resistance. Symbols are explained in the main text.

kinetic term, i.e., the denominator of the Michaelis-Menten term in Equation 21 which MMRT does not consider; Arcus et al., 2016; Schipper et al., 2014). Therefore, for a population of cells that are not under substrate limitation and are exponentially growing (so that one metabolic pathway dominates the metabolism), one should expect a MMRT-type temperature dependence of the metabolic rates. This result explains why Ratkowsky et al. (2005) were able to use the following equation to model bacterial growth rates under unlimited substrate supply (where the right-hand side of Equation 21 is reduced to $v_{max,chain}\prod_j f_{ax,j}$):

$$g = \frac{cT\,exp\left(-\Delta H_A/RT\right)}{1 + exp\left(-\frac{n}{RT}\left(\Delta H^* - T\Delta S^* + \Delta C_p\left[\left(T - T_H^*\right) - T\,ln\left(T/T_S^*\right)\right]\right)\right)} \quad (23)$$

where g is growth rate, c is an empirical constant, and ΔH_A is substrate-dependent activation energy. However, unlike previous assumptions that properties of some single control enzyme determine the overall growth (Johnson & Lewin, 1946), here n and ΔC_p represent mean values of protein length and their thermal properties, under possible influences from other molecules, such as phospholipids (e.g., Mansy & Szostak, 2008).

In summary, for dynamic modeling of microbial substrate uptake and assimilation (and perhaps plant autotrophic respiration as well, e.g., Liang et al., 2018), we recommend representing the temperature sensitivity as in Equation 21 rather than using the MMRT directly. Additionally, we note that plant photosynthesis models have long represented carboxylation and oxygenation using a form similar to Equation 21 (e.g., Medlyn et al., 2002). Adopting a similar functional form for microbial biogeochemical reactions (and plant autotrophic respiration) may improve the coherence of coupled plant-soil-microbe interactions. Besides, the Ohm's law formulation above will further enable biogeochemical models to use proteomic information to inform their parameterization that is not possible with the Michaelis-Menten kinetics.

3.2. Series Resistor-Based Formulation of Enzyme-Catalyzed Redox Reactions

Many biogeochemical processes are of the redox type, for example, photosynthesis, aerobic respiration, nitrification, and anaerobic denitrification (Madigan et al., 2009; Taiz & Zeiger, 2006). Basically, enzyme-catalyzed redox reactions facilitate electron transfers from electron donors to electron acceptors. This process can be summarized with the schema in Figure 2a that has one resistor representing electron donors ($r_{S,edon}$),

and the other resistor ($r_{S,eacc}$) representing electron acceptors, with the enzyme (symbolically) being the battery. By applying the Ohm's law analogy, the reaction rate is

$$v = \frac{E}{r_{eacc} + r_{edon}} \tag{24}$$

where $r_{eacc} = \left(1/v_{max,eacc}\right) + \left(1/k_{f,eacc}S_{eacc}\right)$, and $r_{edon} = \left(1/v_{max,edon}\right) + \left(1/k_{f,edon}S_{edon}\right)$. When the two are combined, Equation 24 can be rewritten as

$$v = \frac{E}{r_E + \left(1/k_{f,eacc}S_{eacc}\right) + \left(1/k_{f,edon}S_{edon}\right)} \tag{25}$$

with $r_E = \left(1/v_{max,eacc}\right) + \left(1/v_{max,edon}\right)$, $r_{S,eacc} = 1/k_{f,eacc}S_{eacc}$, and $r_{S,edon} = 1/k_{f,edon}S_{edon}$. We note that in this series resistor-based formulation, the total resistance (or mean first passage time) does not include the discount resulting from the concurrent binding of electron donors and acceptors to the enzyme (i.e., type-2 configuration in Figure 2b, where electron donor binds before electron acceptor to the enzyme, is as good as type-1 configuration in Figure 2a, where electron donor binds after electron acceptor to the enzyme; because these two configurations have the same resistance, they are not differentiated in the Ohm's law analogy). However, this discount can be incorporated by renewal theory (or law of mass action, where these two configurations are considered as different and allowed to occur concurrently, such that the total resistance is smaller), which leads to the synthesizing unit (SU) model (Kooijman, 1998) below:

$$v = \frac{E}{r_E + \left(1/k_{f,eacc}S_{eacc}\right) + \left(1/k_{f,edon}S_{edon}\right) - \left(1/k_{f,eacc}S_{eacc} + k_{f,edon}S_{edon}\right)} \tag{26}$$

Compared to Equation 25, the SU model (i.e., Equation 26) is numerically more accurate (in approximating the law of mass action, the standard method that deals with biogeochemical reactions, Koudriavstev et al., 2001). Equations 25 and 26 differ by the term $-1/\left(k_{f,eacc}S_{eacc} + k_{f,edon}S_{edon}\right)$ that accounts for the coexistence of schemas in Figures 2a and 2b.

Equation 25 was derived as early as in Alberty (1953) and is called the additive model. It was found to be the superior formulation to model multiple nutrient limitations of microbial and plant growth in O'Neill et al. (1989) (where electron donors and acceptors are replaced with complementary nutrients, such as nitrogen and phosphorus). In particular, the additive model (Equation 25) can be extended to include an arbitrary number of nutrients:

$$v = \frac{E}{r_E + \sum_j \left(1/k_{f,j}S\right)} \tag{27}$$

where S_j are essential nutrients (e.g., carbon, nitrogen, phosphorus, potassium, and chloronium). Smith (1976, 1979) used Equation 27 to model plant growth and microbial growth under carbon, nitrogen, phosphorus, and potassium colimitation. Based on past successful applications (Franklin et al., 2011; Kooijman, 1998), the SU model (i.e., Equation 26) may be argued as mathematically more rigorous than the series resistor-based additive model (i.e., Equation 25 or 27). However, given the usually significant uncertainty of ecological data, the series resistor-based additive model may be equally good (even using the same parameters as in the SU model). Indeed, when we applied both the SU model and the resistor-based additive model to the measured algal growth rates under various levels of phosphorus and vitamin B_{12} additions (Droop, 1974; this data set was also used by Kooijman (1998) when the SU model was first developed), both models can be satisfyingly calibrated with respect to the growth data (Figures 3a and 3b; albeit higher maximum growth rate is inferred for fast adapted algae by the SU model, Table S1 in Supporting Information S1). Nevertheless, when the normalized growth rates are plotted as a function of the normalized substrate fluxes, the SU and resistor-based additive models show very similar growth patterns (Figures 3c and 3d). The SU model and additive model also performed equally well for the plant growth data from Shaver and Melillo (1984) (Figure 4), and their parameter values are also quite comparable in magnitude (Figure S1 and Table S1 in Supporting Information S1). Moreover, when the SU and additive models are used to model aerobic heterotrophic respiration using the parameterization from Tang and Riley (2019a), we once again find the two models driven by identical parameters resulted in very similar goodness of fit with respect to the measurements (Figure 5 and Table S2 in Supporting Information S1). These lines of evidence suggest that one can probably use these two models alternatively (but more extensive studies are needed to quantify the resultant structural uncertainty in the broader context of biogeochemical modeling). In particular, both

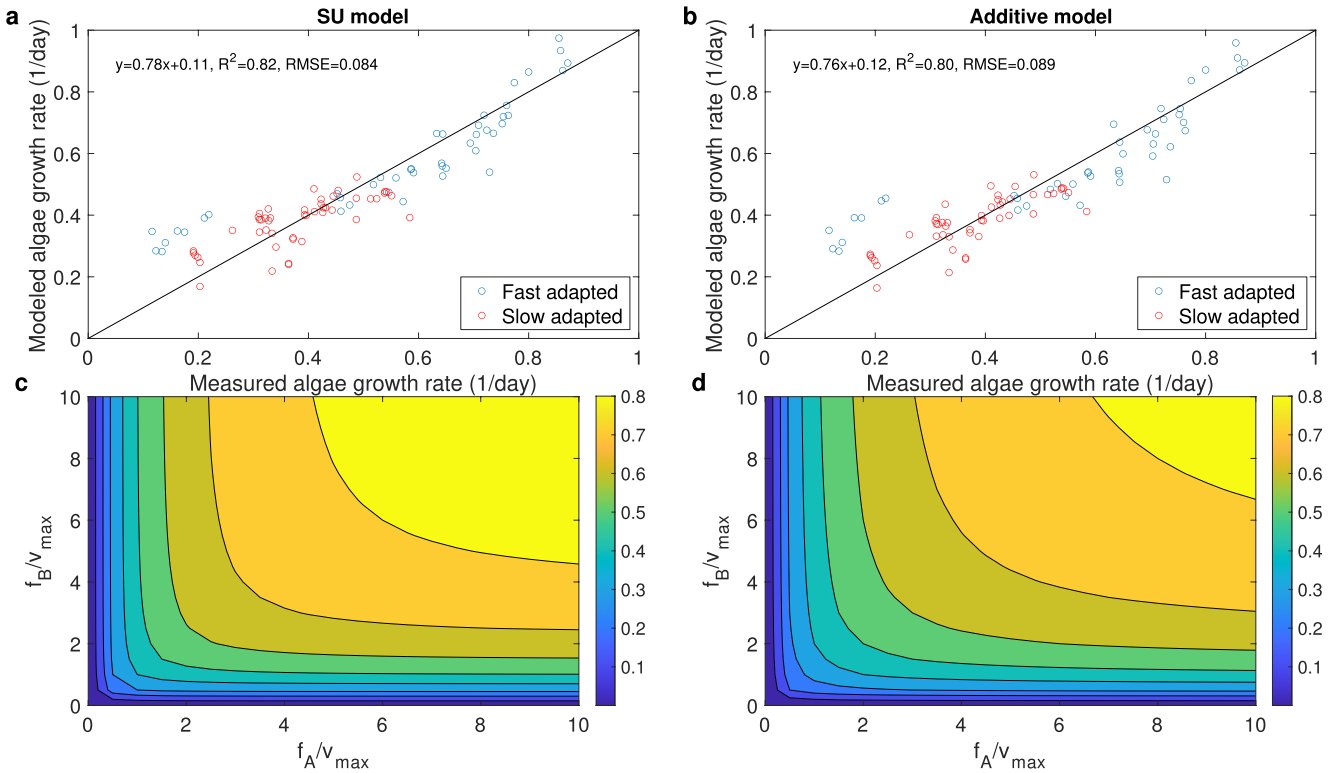

Figure 3. (a) Comparison of the calibrated synthesizing unit (SU) model prediction for the algal growth rates data from Droop (1974); Panel (b) same as panel (a) but from the calibrated resistor-based additive model; (c) Contour of normalized growth rate as a function of normalized fluxes of substrates A (with $f_A = k_{f,A}S_A$) and B (with $f_B = k_{f,B}S_B$) for the SU model; Panel (d) same as panel (c) but for the resistor-based additive model. The additive model is presented as Equation 25, and the SU model is presented as Equation 26. Model parameters are in Table S1 in Supporting Information S1.

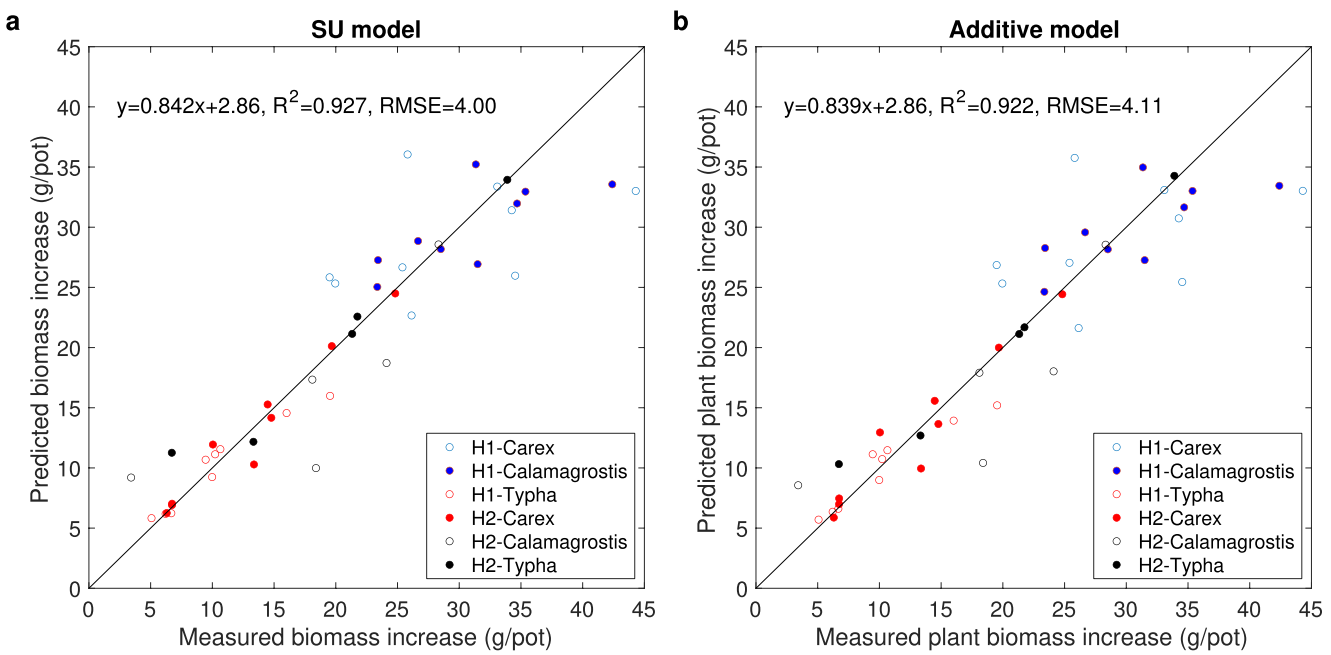

Figure 4. (a) SU model predicted versus measured plant growth; (b) Additive model predicted versus measured plant growth. The data are from Shaver and Melillo (1984). Model parameters are in Table S1 in Supporting Information S1.

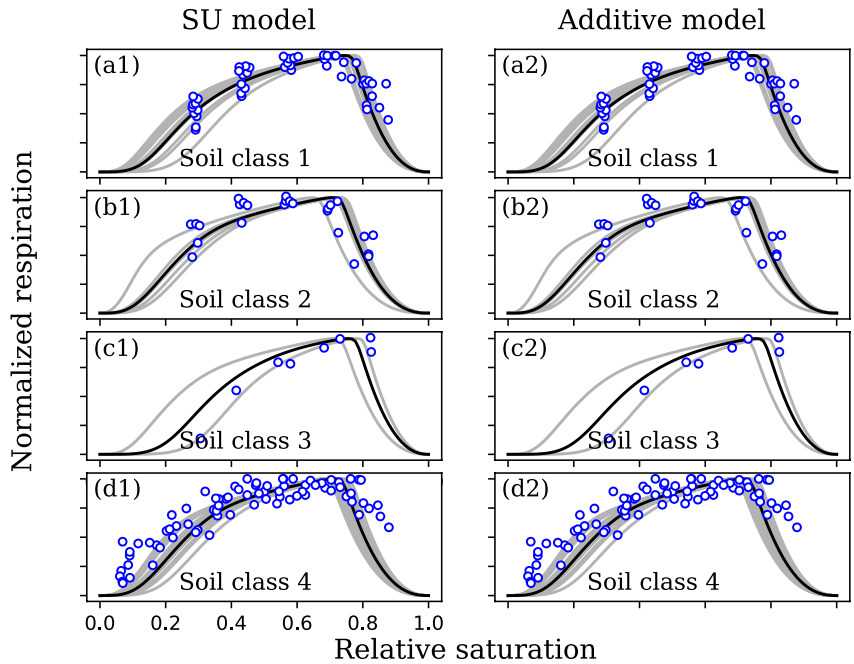

Figure 5. Left panels are SU model-based prediction of respiration-soil-moisture relationship; right panels are based on the resistor-based additive model. The two models (described in Supporting Information S1) used identical parameters, which are detailed in Tang and Riley (2019a). The statistics for model-data fitting (in terms of linear regression and root mean square error) between two models are identical to 0.01 (see Table S2 in Supporting Information S1).

can be a substitute for Liebig's law of the minimum that is used by most existing biogeochemical models (Achat et al., 2016; Tang & Riley, 2021). However, the additive model (derived from the Ohm's law analogy) is computationally much simpler than the theoretically more accurate SU model for situations that involve many more complementary nutrients (Tang & Riley, 2021).

Additionally, we note that Equation 27 can be extended (using a mixed series-parallel circuit; see Figure 6b and Section 3.4) into a photosynthesis model to replace the Farquhar or Collatz model that is formulated based on Liebig's law of the minimum, which has to arbitrarily smooth the abrupt transitions from one limiting process to another (e.g., Collatz et al., 1990, 1992; Farquhar et al., 1980; Kirschbaum & Farquhar, 1984). Notably, the use of Liebig's law of the minimum and smoothing functions has been recently identified as one major source of uncertainty in modeling terrestrial ecosystem gross primary productivity (Walker et al., 2021). Taking these potential applications together, we contend that it is possible to use the same kinetics to formulate models of plant photosynthesis, microbial substrate dynamics, and biomass growth, a strategy that will likely enhance the mathematical coherence in modeling plant-soil-microbe interactions.

3.3. Parallel Resistor-Based Formulation of Competitive Kinetics

Many microorganisms can feed on multiple substrates. For example, *Escherichia coli* and yeasts are able to perform both aerobic and anaerobic respiration (e.g., Dashko et al., 2014; Unden & Bongaerts, 1997); some methanotrophic bacteria can oxidize methane, ammonia, and carbon monoxide (Bedard & Knowles, 1989); and some denitrifiers can consume oxygen, nitrate, nitrite, nitric oxide, and nitrous oxide while feeding on one carbon substrate (Chen & Strous, 2013). Plants can also use diverse mineral nitrogen forms to produce biomass (e.g., Masclaux-Daubresse et al., 2010; Tang & Riley, 2021). Moreover, some enzymes can react on different substrates. For example, the ribonuclease enzyme is able to degrade various RNA molecules (Etienne et al., 2020). One common feature shared by all these different biogeochemical processes is that the uptake of one substrate often competitively inhibits the uptake of others. Thus, it is meaningful for us to show that such problems can be formulated using the parallel circuit (plus one series resistor) using the Ohm's law analogy.

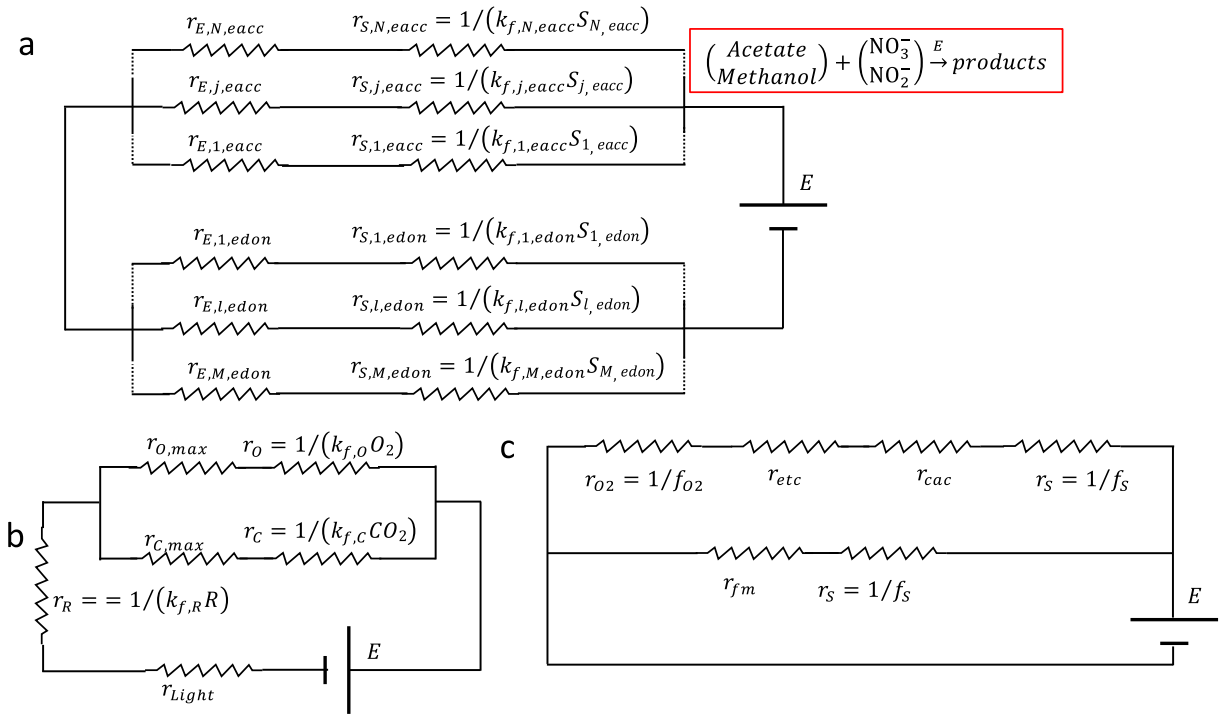

Figure 6. (a) Mixed resistor circuit schema for redox reactions with alternative electron donors and acceptors, with example (in red box) depicting the use of acetate and methanol as electron donors, and nitrite and nitrate as electron acceptors during denitrification; (b) Circuit scheme for photosynthesis; (c) Circuit schema for the parallel fermentation and aerobic respiration pathways. Symbols are explained in the main text.

We first formulate the competitive Michaelis-Menten kinetics using the schema in Figure 2c. For this case, the total resistance is

$$r = r_E + r_S = r_E + \left(\sum_j \left(r_{E,j} + r_{S,j}\right)^{-1}\right)^{-1} \tag{28}$$

where $r_{S,j}{}^{-1} = k_{f,j}S_j$, and $r_{E,j}$ is the resistance due to preprocessing of substrate S_j before it is handed to the central enzyme E (i.e., the enzyme that products of all substrates have to pass through), and $r_E = 1/v_{max,E}$ is the resistance due to the maximum substrate processing rate of the central enzyme (which for redox reactions could be determined by the time spent on processing the electron donors if S_j here are electron acceptors). If $r_{E,j} = 0$, which is usually assumed for competitive Michaelis-Menten kinetics, the second term r_S becomes $\left(\sum_j k_{f,j}S_j\right)^{-1}$, and the reaction velocity is

$$v = \frac{E}{r} = \frac{E}{\left(1/v_{max}\right) + \left(\sum_j k_{f,j}S_j\right)^{-1}} \tag{29}$$

and the corresponding flux through pathway j is

$$v_j = \frac{vr_S}{r_{S,j}} = v\frac{k_{f,j}S_j}{\sum_l k_{f,l}S_l} = E \cdot \frac{v_{max}S_j/K_j}{1 + \sum_l S_l/K_l} \tag{30}$$

where $K_j = v_{max}/k_{f,j}$. Therefore, v_j is the reaction velocity computed from the competitive Michaelis-Menten kinetics. We note that Equation 30 is meaningful only when pathway j produces new molecules. However, even for inhibitors, whose binding to enzymes does not produce new molecules, if we regard dissociation as a way of producing new molecules, then Equation 30 is still meaningfully representing competitive inhibition.

3.4. Mixed Series and Parallel Resistor-Based Formulation of Redox Reactions of Alternative Electron Donors and Acceptors

Many microorganisms (such as denitrifying bacteria that play an essential role in the Earth's nitrogen cycle; e.g., Robertson & Groffman, 2015) are able to grow on different electron donors and acceptors. Such processes can be modeled using the SUPECA kinetics (Tang & Riley, 2017). Below, we show that it can also be formulated using the schema of mixed series and parallel resistors in the Ohm's law framework.

Based on the schema in Figure 6a, the total resistance is

$$r = r_{edon} + r_{eacc} = \left(\sum_l r_{l,edon}{}^{-1}\right)^{-1} + \left(\sum_j r_{j,eacc}{}^{-1}\right)^{-1} \tag{31}$$

where the resistance for electron donors is

$$r_{l,edon} = r_{E,l,edon} + r_{S,l,edon} = \frac{1}{v_{max,l,edon}} + \frac{1}{k_{f,l,edon} S_{l,edon}} \tag{32}$$

and the resistance for electron acceptors is

$$r_{j,eacc} = r_{E,j,eacc} + r_{S,j,eacc} = \frac{1}{v_{max,j,eacc}} + \frac{1}{k_{f,j,eacc} S_{j,eacc}} \tag{33}$$

Accordingly, the corresponding reaction flux through electron donor j is

$$v_{j,edon} = \frac{E}{r}\frac{r_{edon}}{r_{j,edon}} = \frac{E}{r_{j,edon}}\frac{r_{edon}}{r_{edon} + r_{eacc}} \tag{34}$$

while the corresponding reaction flux through electron acceptor j is

$$v_{j,eacc} = \frac{E}{r}\frac{r_{eacc}}{r_{j,eacc}} = \frac{E}{r_{j,eacc}}\frac{r_{eacc}}{r_{edon} + r_{eacc}} \tag{35}$$

Now considering an application that involves two electron acceptors, for example, nitrate and nitrite in denitrification, we have

$$\frac{1}{r_{eacc}} = \frac{1}{r_{NO_3}} + \frac{1}{r_{NO_2}} \tag{36}$$

which when combined with Equation 35 leads to

$$v_{NO_3} = \frac{E}{r_{NO_3} + r_{edon} + r_{edon} r_{NO_3}/r_{NO_2}} \tag{37}$$

and

$$v_{NO_2} = \frac{E}{r_{NO_2} + r_{edon} + r_{edon} r_{NO_2}/r_{NO_3}} \tag{38}$$

which are just Equation 10 in Almeida et al. (1997) that have been successfully used to fit the measurement of denitrification rates from Almeida et al. (1995). With proper number of resistors, the denitrifier model by Domingo-Felez and Smets (2020) can also be easily recovered from Equations 31–35.

Further, we note that the relationship between the light, Rubisco enzyme-catalyzed carboxylation and oxygenation reactions in photosynthesis can be formulated analogously in Figure 6b, from which we can obtain the gross carbon fixation rate A_g as

$$A_g = \frac{E r_{OC}}{r_{Light} + r_R + r_{OC}}\left(\frac{1}{r_{C,max} + r_C} - \frac{0.5}{r_{O,max} + r_O}\right) \tag{39}$$

where

$$r_{OC} = \left(\frac{1}{r_{C,max} + r_C} + \frac{1}{r_{O,max} + r_O}\right)^{-1} \tag{40}$$

with E representing Rubisco enzyme, r_{Light} is due to light reaction, r_R is due to RuBP flux, $r_{C,max}$ and r_C are associated with the carboxylation pathway, and $r_{O,max}$ and r_O are associated with the oxygenation pathway. However, we will present detailed quantitative analysis elsewhere.

In summary, the examples in Sections 3.1–3.4 show that the Ohm's law analogy can formulate both plant and microbial biogeochemistry in the same framework.

3.5. Other Potential Applications of the Ohm's Law Analogy

Besides the applications described above, we below derive some quite interesting results to further highlight the potential of the Ohm's law analogy in biogeochemical modeling.

First, we will explain why fermentation can occur even when there is still oxygen to support the energetically more efficient aerobic respiration. Such a phenomenon is called the Warburg effect (i.e., lactate producing aerobic fermentation) in proliferating mammalian cells (a phenomenon important to the understanding of cancer development), or the Crabtree effect (i.e., ethanol fermentation) of unicellular yeast *Saccharomyces cerevisiae* (e.g., de Alteriis et al., 2018). *Escherichia coli* have also been observed to shift to the seemingly bioenergetically less efficient yet faster metabolic pathways under high substrate concentrations (e.g., Flamholz et al., 2013; Labhsetwar et al., 2014). Depending on the details to be represented, we acknowledge that there are multiple ways to model such phenomenon even with the circuit analogy (Molenaar et al., 2009; Schuster et al., 2015), highlighting the challenge for a comprehensive and robust understanding of this biochemical phenomenon. We next present one plausible mathematical explanations to show that, under certain aerobic conditions, high glucose concentration makes fermentation more favorable.

According to the schema in Figure 6c, the specific ATP generation rate from the fermentation pathway is

$$v_{FM,ATP} = \frac{Y_{FM}}{\left(1/f_S\right) + r_{fm}} \tag{41}$$

where f_S is the incoming flux of pyruvate (produced from glycolysis) sensed by the two metabolic pathways (and is proportional to the incoming glucose flux sensed by the organism under steady state), r_{fm} is the resistance associated with the conversion of pyruvate into fermentation products (which could be lactate, ethanol, or acetate depending on the organism, Madigan et al., 2009), and Y_{FM} is the ATP yield of fermentation. Similarly, the specific ATP generation rate from the aerobic respiration pathway is

$$v_{AO,ATP} = \frac{Y_{AO}}{\left(1/f_S\right) + r_{cac} + r_{etc} + \left(1/f_{O_2}\right)} \tag{42}$$

where r_{acc} and r_{etc} are resistance associated with the citric acid cycle, and the electron transport chain, respectively, while f_{O_2} is the incoming oxygen flux, and Y_{AO} is the ATP yield of aerobic respiration. Because the citric acid cycle involves many more enzyme-catalyzed steps than fermentation, $r_{cac} > r_{fm}$. Meanwhile, Y_{AO} is about 20 times the value of Y_{fm} (Madigan et al., 2009).

In a metabolically active organism, for fermentation to be more favorable than aerobic respiration (in terms of ATP production rate for the same amount of enzyme allocated, i.e., $v_{FM,ATP} > v_{AO,ATP}$), the following condition needs to be satisfied:

$$\frac{Y_{FM}}{Y_{AO}} > \frac{\left(1/f_S\right) + r_{fm}}{\left(1/f_S\right) + r_{cac} + r_{etc} + \left(1/f_{O_2}\right)} > \frac{r_{fm}}{r_{cac} + r_{etc} + \left(1/f_{O_2}\right)} \tag{43}$$

where the term after the second ">" suggests that fermentation is more favorable only when oxygen is below a certain level of availability (note that f_{O_2} is approximately proportional to diffusion). When the oxygen availability is sufficiently low (even though the system is not qualified as anaerobic), higher substrate concentration (i.e., greater f_S) will make fermentation more effective in generating ATP for the same amount of enzyme allocated for catabolic reaction. If we additionally consider that the fermentation pathway requires the organism to maintain a much smaller number of enzymes than required for the aerobic oxidation pathway (which is equivalent to increase the value of Y_{FM}/Y_{AO} further, making the inequality (Equation 43) even easier to be satisfied), we can expect fermentation to be preferred under high glucose supply (i.e., greater f_S) even under certain aerobic conditions. (For anaerobic conditions, f_{O_2} approaches zero, and the inequality (Equation 43) is easily satisfied.)

Therefore, as illustrated above, the Ohm's law analogy enables us to quickly and vividly infer that increasing the substrate concentration S reduces the resistance faster for the fermentation pathway than for the aerobic respiration pathway. Since genomic expression usually follow the induction and then response paradigm

(i.e., the Jacob-Monod model, Tiwari et al., 1974), the microbes under consideration will metabolically shift toward fermentation even though oxygen is available and aerobic respiration yields more ATP per unit of carbon consumed (Causton et al., 2001). In contrast, models based on the flux balance method or law of mass action will be more sophisticated to formulate and understand for such metabolic shift (Kesten et al., 2015; Nilsson & Nielsen, 2016). Given the significance of metabolic shift in various contexts, including methane and hydrogen dynamics in environment and industrial biogeochemistry (Lu et al., 2009; Madigan et al., 2009), we expect to study this problem in a more quantitative and extensive way elsewhere.

Another very interesting application of the Ohm's law analogy is to qualitatively explain why the substrate-growth rate relationship of an exponentially growing bacterial population can be fitted with the Monod kinetics (Monod, 1949), whose validity is assumed implicitly in most existing studies of microbial growth on single substrate. For an exponentially growing bacterial population, the bacteria proteomes are approximately in steady state. Meanwhile, from the Ohm's law analogy, we know that any functioning circuit-network can be equivalently represented by a bulk resistor. Therefore, we contend that however complex the circuit representation of a bacterial metabolism would be, as a whole it can be equivalently represented by a constant resistance r_E. When this r_E is combined with the resistance associated with the incoming substrate flux (see Equation 7), we then say that the bacterial growth would very likely follow the Monod kinetics. However, when the bacteria are in transition from one metabolic state into another (e.g., from gluconate to succinate), extra resistors are introduced accompanying the change of proteomes, resulting in a dynamic r_E and thus Monod kinetics will fail for such situations (e.g., Erickson et al., 2017). This argument also explains why models based on flux balance analysis with proteomic constraints can simulate exponentially growing *E. coli* and yeast realistically (Labhsetwar et al., 2014, 2017), but the flux balance models are cumbersome to apply in dynamic environments.

3.6. Limitations of the Ohm's Law Analogy

While the Ohm's law analogy can be used to model many challenging biogeochemical processes, it is not appropriate for all types of biogeochemical networks. For instance, it is not able to properly couple two or more consumers (i.e., two or more batteries) within a single circuit network, even though the electric circuit theory itself does not forbid such a configuration to occur (which can be solved with the Kirchhoff's law of voltage and current, e.g., Feynman et al., 2011b). Rather, the coupling can only be done by first representing the substrate dynamics of each consumer separately, and then coupling them together by differential equations. Such coupling could be critical when many consumers are competing for a limiting substrate, even though none of the consumers is substrate limited when other consumers are excluded (e.g., Etienne et al., 2020). The ECA kinetics (Tang & Riley, 2013b) and its progeny SUPECA kinetics (Tang & Riley, 2017) are more capable of resolving such situations. In soil biogeochemistry, one such situation is to model the interaction of a substrate molecule (e.g., ammonium, inorganic phosphorus, or dissolved organic carbon) that is simultaneously undergoing uptake by organisms and adsorption by mineral surfaces. Fortunately, a simple remedy is possible for the Ohm's law analogy from the ECA kinetics. In the ECA kinetics, microbial uptake of substrate S under the influence of adsorption by mineral surface M (with affinity parameter K_M) is

$$F = \frac{v_{max} SB}{K + S + MK/K_M + \alpha B} \tag{44}$$

where K is the half saturation constant for the uptake of S by microbe B in the absence of M, and αB is the within-population competition effect introduced by ECA. Tang and Riley (2019b) showed that αB is negligible due to the large size contrast between microbes (and likewise fine roots) and substrate molecules. When αB is ignored, Equation 44 becomes

$$F = \frac{B}{\left(1/v_{max}\right) + \left(1/k_f S\right)\left(1 + \left(M/K_M\right)\right)} = \frac{B}{\left(1/v_{max}\right) + \left(1/k_f^* S\right)} \tag{45}$$

with

$$k_f^* = \frac{k_f}{1 + \left(M/K_M\right)} \tag{46}$$

Now the Ohm's law analogy will still work if $1/k_f^* S$ is used to defined the substrate-dependent resistance. Moreover, Equation 46 suggests that mineral surfaces may slow the microbial uptake of substrate S by effectively reducing the substrate delivery rate toward the microbes.

However, when the sizes of substrates and competitors are similar (e.g., in some predator-prey relationships), the Ohm's law analogy will be too cumbersome to apply, and the ECA or SUPECA kinetics should be used. Nonetheless, it will be very interesting and helpful to construct and compare models for the same system using both the Ohm's law analogy and ECA (or SUPECA) kinetics.

4. Conclusions

By exploiting the mathematical similarity between the Ohm's law and Michaelis-Menten kinetics, we show that the electric circuit analogy can be used to derive many interesting results of biogeochemical kinetics. We show this approach reproduces many successful applications in the literature, including aerobic heterotrophic respiration, multinutrient colimited microbial (and plant) growth, and denitrification dynamics. This approach also sheds new insights on the temperature sensitivity of kinetic parameters in substrate uptake, the Warburg and Crabtree effect in prokaryotes and eukaryotes, and conceptually explains why the Monod relationship accurately represents the kinetics of exponentially growing bacterial populations, and why flux balance modeling constrained by proteomics is able to accurately model microbial growth. Based on these results, we expect that the Ohm's law analogy will help build a unified kinetic modeling framework of microbial and plant biogeochemistry to make more robust predictions.

Conflict of Interest

The authors declare no conflicts of interest relevant to this study.

Data Availability Statement

Data are available through Shaver and Melillo (1984), Droop (1974), Franzluebbers (1999), and Doran et al. (1990).

Acknowledgments
This research was supported by the Director, Office of Science, Office of Biological and Environmental Research of the US Department of Energy under contract no. DE-AC02-05CH11231 as part of the Next Generation Ecosystem Experiment-Arctic project and the Energy Exascale Earth System Model (E3SM) project for J. Y. Tang and W. J. Riley, the TES Soil Warming SFA for W. J. Riley, and the Department of Energy, Office of Biological and Environmental Research, Genomic Sciences Program through the LLNL Microbes Persist Science Focus Area for GLM. E. L. Brodie was supported by funding from the Department of Energy, Office of Biological and Environmental Research, Subsurface Biogeochemical Research Program through the LBNL Watershed Function Science Focus Area. Financial support does not constitute an endorsement by the Department of Energy of the views expressed in this study.

References

Achat, D. L., Augusto, L., Gallet-Budynek, A., & Loustau, D. (2016). Future challenges in coupled C-N-P cycle models for terrestrial ecosystems under global change: A review. *Biogeochemistry*, *131*(1–2), 173–202. https://doi.org/10.1007/s10533-016-0274-9

Alberty, R. A. (1953). The relationship between Michaelis constants, maximum velocities and the equilibrium constant for an enzyme-catalyzed reaction. *Journal of the American Chemical Society*, *75*(8), 1928–1932. https://doi.org/10.1021/ja01104a045

Alberty, R. A., & Hammes, G. G. (1958). Application of the theory of diffusion-controlled reactions to enzyme kinetics. *The Journal of Physical Chemistry*, *62*(2), 154–159. https://doi.org/10.1021/j150560a005

Aledo, J. C., & del Valle, A. E. (2002). Glycolysis in wonderland: The importance of energy dissipation in metabolic pathways. *Journal of Chemical Education*, *79*(11), 1336–1339. https://doi.org/10.1021/ed079p1336

Allison, S. D., Romero-Olivares, A. L., Lu, Y., Taylor, J. W., & Treseder, K. K. (2018). Temperature sensitivities of extracellular enzyme V_{max} and K_m across thermal environments. *Global Change Biology*, *24*(7), 2884–2897. https://doi.org/10.1111/gcb.14045

Almeida, J. S., Reis, M. A. M., & Carrondo, M. J. T. (1995). Competition between nitrate and nitrite reduction in denitrification by *Pseudomonas fluorescens*. *Biotechnology and Bioengineering*, *46*(5), 476–484. https://doi.org/10.1002/bit.260460512

Almeida, J. S., Reis, M. A. M., & Carrondo, M. J. T. (1997). A unifying kinetic model of denitrification. *Journal of Theoretical Biology*, *186*(2), 241–249. https://doi.org/10.1006/jtbi.1996.0352

Alster, C. J., von Fischer, J. C., Allison, S. D., & Treseder, K. K. (2020). Embracing a new paradigm for temperature sensitivity of soil microbes. *Global Change Biology*, *26*(6), 3221–3229. https://doi.org/10.1111/gcb.15053

Arcus, V. L., Prentice, E. J., Hobbs, J. K., Mulholland, A. J., Van der Kamp, M. W., Pudney, C. R., et al. (2016). On the temperature dependence of enzyme-catalyzed rates. *Biochemistry*, *55*(12), 1681–1688. https://doi.org/10.1021/acs.biochem.5b01094

Atkins, P., Jones, L., & Laverman, L. (2016). *Chemical principles: The quest for insight* (7th ed.). W. H. Freeman.

Bedard, C., & Knowles, R. (1989). Physiology, biochemistry, and specific inhibitors of CH_4, NH_4^+, and CO oxidation by methanotrophs and nitrifiers. *Microbiological Reviews*, *53*(1), 68–84. https://doi.org/10.1128/mr.53.1.68-84.1989

Bonan, G. (2019). *Climate change and terrestrial ecosystem modeling*. Cambridge University Press. https://doi.org/10.1017/9781107339217

Briggs, G. E., & Haldane, J. B. S. (1925). A note on the kinetics of enzyme action. *Biochemical Journal*, *19*(2), 338–339. https://doi.org/10.1042/bj0190338

Brutsaert, W. (2005). *Hydrology: An introduction*. Cambridge University Press.

Cao, J. S. (2011). Michaelis–Menten equation and detailed balance in enzymatic networks. *The Journal of Physical Chemistry B*, *115*(18), 5493–5498. https://doi.org/10.1021/jp110924w

Causton, H. C., Ren, B., Koh, S. S., Harbison, C. T., Kanin, E., Jennings, E. G., et al. (2001). Remodeling of yeast genome expression in response to environmental changes. *Molecular Biology of the Cell*, *12*(2), 323–337. https://doi.org/10.1091/mbc.12.2.323

Chen, J. W., Hanke, A., Tegetmeyer, H. E., Kattelmann, I., Sharma, R., Hamann, E., et al. (2017). Impacts of chemical gradients on microbial community structure. *The ISME Journal*, *11*(4), 920–931. https://doi.org/10.1038/ismej.2016.175

Chen, J. W., & Strous, M. (2013). Denitrification and aerobic respiration, hybrid electron transport chains and co-evolution. *Biochimica et Biophysica Acta: Bioenergetics*, *1827*(2), 136–144. https://doi.org/10.1016/j.bbabio.2012.10.002

Chou, K. C., & Jiang, S. P. (1974). Studies on the rate of diffusion-controlled reactions of enzymes: Spatial factor and force field factor. *Scientia Sinica*, *XVII*(5). https://doi.org/10.1360/ya1974-17-5-664

Collatz, G. J., Berry, J. A., Farquhar, G. D., & Pierce, J. (1990). The relationship between the rubisco reaction-mechanism and models of photosynthesis. *Plant, Cell and Environment*, *13*(3), 219–225. https://doi.org/10.1111/j.1365-3040.1990.tb01306.x

Collatz, G. J., Ribas-Carbo, M., & Berry, J. A. (1992). Coupled photosynthesis-stomatal conductance model for leaves of C4 plants. *Australian Journal of Plant Physiology*, *19*(5), 519–538. https://doi.org/10.1071/PP9920519

Cramer, J. S. (2002). *The origins of logistic regression*. University of Amsterdam and Tinbergen Institute.

Dashko, S., Zhou, N., Compagno, C., & Piskur, J. (2014). Why, when, and how did yeast evolve alcoholic fermentation? *FEMS Yeast Research*, *14*(6), 826–832. https://doi.org/10.1111/1567-1364.12161

Davidson, E. A., Samanta, S., Caramori, S. S., & Savage, K. (2012). The Dual Arrhenius and Michaelis-Menten kinetics model for decomposition of soil organic matter at hourly to seasonal time scales. *Global Change Biology*, *18*(1), 371–384. https://doi.org/10.1111/j.1365-2486.2011.02546.x

de Alteriis, E., Carteni, F., Parascandola, P., Serpa, J., & Mazzoleni, S. (2018). Revisiting he Crabtree/Warburg effect in a dynamic perspective: A fitness advantage against sugar-induced cell death. *Cell Cycle*, *17*(6), 688–701. https://doi.org/10.1080/15384101.2018.1442622

Dill, K. A., Ghosh, K., & Schmit, J. D. (2011). Physical limits of cells and proteomes. *Proceedings of the National Academy of Sciences of the United States of America*, *108*(44), 17876–17882. https://doi.org/10.1073/pnas.1114477108

Domingo-Felez, C., & Smets, B. F. (2020). Modeling denitrification as an electric circuit accurately captures electron competition between individual reductive steps: The Activated Sludge Model-Electron Competition model. *Environmental Science & Technology*, *54*(12), 7330–7338. https://doi.org/10.1021/acs.est.0c01095

Doob, J. L. (1948). Renewal theory from the point of view of the theory of probability. *Transactions of the American Mathematical Society*, *63*, 422–438. https://doi.org/10.1090/S0002-9947-1948-0025098-8

Doran, J. W., Mielke, L. N., & Power, J. F. (1990). *Microbial activity as regulated by soil water-filled pore space*. International Society of Soil Science.

Droop, M. R. (1974). Nutrient status of algal cells in continuous culture. *Journal of the Marine Biological Association of the United Kingdom*, *54*(4), 825–855. https://doi.org/10.1017/S002531540005760x

English, B. P., Min, W., van Oijen, A. M., Lee, K. T., Luo, G. B., Sun, H. Y., et al. (2006). Ever-fluctuating single enzyme molecules: Michaelis-Menten equation revisited. *Nature Chemical Biology*, *2*(2), 87–94. https://doi.org/10.1038/nchembio759

Erickson, D. W., Schink, S. J., Patsalo, V., Williamson, J. R., Gerland, U., & Hwa, T. (2017). A global resource allocation strategy governs growth transition kinetics of *Escherichia coli*. *Nature*, *551*(7678), 119–123. https://doi.org/10.1038/nature24299

Etienne, T. A., Cocaign-Bousquet, M., & Ropers, D. (2020). Competitive effects in bacterial mRNA decay. *Journal of Theoretical Biology*, *504*, 110333. https://doi.org/10.1016/j.jtbi.2020.110333

Eyring, H. (1935). The activated complex and the absolute rate of chemical reactions. *Chemical Reviews*, *17*(1), 65–77. https://doi.org/10.1021/cr60056a006

Farquhar, G. D., Caemmerer, S. V., & Berry, J. A. (1980). A biochemical-model of photosynthetic CO_2 assimilation in leaves of C3 species. *Planta*, *149*(1), 78–90. https://doi.org/10.1007/BF00386231

Feynman, R. P., Leighton, R. B., & Sands, M. (2011a). *The Feynman lectures on physics, Vol. I: Mainly mechanics, radiation, and heat* (New Millennium ed.). Basic Books.

Feynman, R. P., Leighton, R. B., & Sands, M. (2011b). *The Feynman lectures on physics, Vol. II: Mainly electromagnetism and matter* (New Millennium ed.). Basic Books.

Feynman, R. P., Leighton, R. B., & Sands, M. (2011c). *The Feynman lectures on physics, Vol. III: Quantum mechanics* (New Millennium ed.). Basic Books.

Flamholz, A., Noor, E., Bar-Even, A., Liebermeister, W., & Milo, R. (2013). Glycolytic strategy as a tradeoff between energy yield and protein cost. *Proceedings of the National Academy of Sciences of the United States of America*, *110*(24), 10039–10044. https://doi.org/10.1073/pnas.1215283110

Franklin, O., Hall, E. K., Kaiser, C., Battin, T. J., & Richter, A. (2011). Optimization of biomass composition explains microbial growth-stoichiometry relationships. *The American Naturalist*, *177*(2), E29–E42. https://doi.org/10.1086/657684

Franzluebbers, A. J. (1999). Microbial activity in response to water-filled pore space of variably eroded southern Piedmont soils. *Applied Soil Ecology*, *11*(1), 91–101. https://doi.org/10.1016/S0929-1393(98)00128-0

Frederiksen, K. B., & Andresen, B. (2008). Mitochondrial optimization using thermodynamic geometry. In G. S. Natarajan, A. A. Bhalekar, & S. S. Dhondge (Eds.), *Recent advances in thermodynamic research including nonequilibrium thermodynamics* (pp. 10–14). Nagpur University.

Garcia-Colin, L. S., del Castillo, L. F., & Goldstein, P. (1989). Theoretical basis for the Vogel-Fulcher-Tammann equation. *Physical Review B: Condensed Matter*, *40*(10), 7040–7044. https://doi.org/10.1103/physrevb.40.7040

Ghosh, K., & Dill, K. (2010). Cellular proteomes have broad distributions of protein stability. *Biophysical Journal*, *99*(12), 3996–4002. https://doi.org/10.1016/j.bpj.2010.10.036

Heinze, C., Eyring, V., Friedlingstein, P., Jones, C., Balkanski, Y., Collins, W., et al. (2019). ESD reviews: Climate feedbacks in the Earth system and prospects for their evaluation. *Earth System Dynamics*, *10*(3), 379–452. https://doi.org/10.5194/esd-10-379-2019

Holling, C. S. (1959). Some characteristics of simple types of predation and parasitism. *The Canadian Entomologist*, *XCI*(7), 385–398. https://doi.org/10.4039/ent91385-7

Jin, Q., & Bethke, C. M. (2007). The thermodynamics and kinetics of microbial metabolism. *American Journal of Science*, *307*(4), 643–677. https://doi.org/10.2475/04.2007.01

Johnson, F. H., & Lewin, I. (1946). The growth rate of *E. coli* in relation to temperature, quinine and coenzyme. *Journal of Cellular and Comparative Physiology*, *28*(1), 47–75. https://doi.org/10.1002/jcp.1030280104

Kari, J., Andersen, M., Borch, K., & Westh, P. (2017). An inverse Michaelis–Menten approach for interfacial enzyme kinetics. *ACS Catalysis*, *7*(7), 4904–4914. https://doi.org/10.1021/acscatal.7b00838

Kesten, D., Kummer, U., Sahle, S., & Hubner, K. (2015). A new model for the aerobic metabolism of yeast allows the detailed analysis of the metabolic regulation during glucose pulse. *Biophysical Chemistry*, *206*, 40–57. https://doi.org/10.1016/j.bpc.2015.06.010
Kirschbaum, M. U. F., & Farquhar, G. D. (1984). Temperature-dependence of whole-leaf photosynthesis in *Eucalyptus pauciflora* Sieb. ex Spreng. *Australian Journal of Plant Physiology*, *11*(6), 519–538. https://doi.org/10.1071/PP9840519
Kooijman, S. A. L. M. (1998). The Synthesizing Unit as model for the stoichiometric fusion and branching of metabolic fluxes. *Biophysical Chemistry*, *73*(1–2), 179–188. https://doi.org/10.1016/S0301-4622(98)00162-8
Kooijman, S. A. L. M. (2009). *Dynamic energy budget theory for metabolic organisation*. Cambridge University Press.
Koudriavstev, A. B., Jameson, R. F., & Linert, W. (2001). *The law of mass action*. Springer. https://doi.org/10.1007/978-3-642-56770-4
Labhsetwar, P., Cole, J. A., Roberts, E., Price, N. D., & Luthey-Schulten, Z. A. (2014). Heterogeneity in protein expression induces metabolic variability in a modeled *Escherichia coli* population (vol 110, pg 14006, 2013). *Proceedings of the National Academy of Sciences of the United States of America*, *111*(2), 876. https://doi.org/10.1073/pnas.1323512111
Labhsetwar, P., Melo, M. C. R., Cole, J. A., & Luthey-Schulten, Z. (2017). Population FBA predicts metabolic phenotypes in yeast. *PLoS Computational Biology*, *13*(9), e1005728. https://doi.org/10.1371/journal.pcbi.1005728
Lane, N., & Martin, W. (2010). The energetics of genome complexity. *Nature*, *467*(7318), 929–934. https://doi.org/10.1038/nature09486
LaRowe, D. E., Dale, A. W., Amend, J. P., & Van Cappellen, P. (2012). Thermodynamic limitations on microbially catalyzed reaction rates. *Geochimica et Cosmochimica Acta*, *90*, 96–109. https://doi.org/10.1016/j.gca.2012.05.011
Lawrence, D. M., Fisher, R. A., Koven, C. D., Oleson, K. W., Swenson, S. C., Bonan, G., et al. (2019). The Community Land Model Version 5: Description of new features, benchmarking, and impact of forcing uncertainty. *Journal of Advances in Modeling Earth Systems*, *11*, 4245–4287. https://doi.org/10.1029/2018MS001583
Liang, L. L., Arcus, V. L., Heskel, M. A., O'sullivan, O. S., Weerasinghe, L. K., Creek, D., et al. (2018). Macromolecular rate theory (MMRT) provides a thermodynamics rationale to underpin the convergent temperature response in plant leaf respiration. *Global Change Biology*, *24*(4), 1538–1547. https://doi.org/10.1111/gcb.13936
Lu, Y., Lai, Q. H., Zhang, C., Zhao, H. X., Ma, K., Zhao, X. B., et al. (2009). Characteristics of hydrogen and methane production from cornstalks by an augmented two- or three-stage anaerobic fermentation process. *Bioresource Technology*, *100*(12), 2889–2895. https://doi.org/10.1016/j.biortech.2009.01.023
Ma, S.-K. (1985). *Statistical mechanics*. World Scientific Publishing Company.
Madigan, M. T., Martinko, J. M., Dunlap, P. V., & Clark, D. P. (2009). *Brock biology of microorganisms* (12th ed.). Pearson Education, Inc.
Maggi, F., Tang, F. H. M., & Riley, W. J. (2018). The thermodynamic links between substrate, enzyme, and microbial dynamics in Michaelis-Menten-Monod kinetics. *International Journal of Chemical Kinetics*, *50*(5), 343–356. https://doi.org/10.1002/kin.21163
Mansy, S. S., & Szostak, J. W. (2008). Thermostability of model protocell membranes. *Proceedings of the National Academy of Sciences of the United States of America*, *105*(36), 13351–13355. https://doi.org/10.1073/pnas.0805086105
Masclaux-Daubresse, C., Daniel-Vedele, F., Dechorgnat, J., Chardon, F., Gaufichon, L., & Suzuki, A. (2010). Nitrogen uptake, assimilation and remobilization in plants: Challenges for sustainable and productive agriculture. *Annals of Botany*, *105*(7), 1141–1157. https://doi.org/10.1093/aob/mcq028
McAdams, H. H., & Shapiro, L. (1995). Circuit simulation of genetic networks. *Science*, *269*(5224), 650–656. https://doi.org/10.1126/science.7624793
Medlyn, B. E., Dreyer, E., Ellsworth, D., Forstreuter, M., Harley, P. C., Kirschbaum, M. U. F., et al. (2002). Temperature response of parameters of a biochemically based model of photosynthesis. II. A review of experimental data. *Plant, Cell and Environment*, *25*(9), 1167–1179. https://doi.org/10.1046/j.1365-3040.2002.00891.x
Michaelis, L., & Menten, M. L. (1913). The kinetics of the inversion effect. *Biochemische Zeitschrift*, *49*, 333–369.
Molenaar, D., van Berlo, R., de Ridder, D., & Teusink, B. (2009). Shifts in growth strategies reflect tradeoffs in cellular economics. *Molecular Systems Biology*, *5*, 323. https://doi.org/10.1038/msb10.1038/msb.2009.82
Monod, J. (1949). The growth of bacterial cultures. *Annual Review of Microbiology*, *3*, 371–394. https://doi.org/10.1146/annurev.mi.03.100149.002103
Murdoch, W. W. (1973). Functional response of predators. *Journal of Applied Ecology*, *10*(1), 335–342.
Murkin, A. S. (2015). Commentary: Ohm's law as an analogy for enzyme kinetics. *Biochemistry and Molecular Biology Education*, *43*(3), 139–141. https://doi.org/10.1002/bmb.20850
Murphy, K. P., Privalov, P. L., & Gill, S. J. (1990). Common features of protein unfolding and dissolution of hydrophobic compounds. *Science*, *247*(4942), 559–561. https://doi.org/10.1126/science.2300815
Nilsson, A., & Nielsen, J. (2016). Metabolic trade-offs in yeast are caused by F1F0-ATP synthase. *Scientific Reports*, *6*. 22264. https://doi.org/10.1038/srep22264
Ninio, J. (1987). Alternative to the steady-state method—Derivation of reaction-rates from 1st-passage times and pathway probabilities. *Proceedings of the National Academy of Sciences of the United States of America*, *84*(3), 663–667. https://doi.org/10.1073/pnas.84.3.663
O'Neill, R. V., Deangelis, D. L., Pastor, J. J., Jackson, B. J., & Post, W. M. (1989). Multiple nutrient limitations in ecological models. *Ecological Modelling*, *46*(3–4), 147–163. https://doi.org/10.1016/0304-3800(89)90015-X
Orth, J. D., Thiele, I., & Palsson, B. O. (2010). What is flux balance analysis? *Nature Biotechnology*, *28*(3), 245–248. https://doi.org/10.1038/nbt.1614
Qian, H. (2008). Cooperativity and specificity in enzyme kinetics: A single-molecule time-based perspective. *Biophysical Journal*, *95*(1), 10–17. https://doi.org/10.1529/biophysj.108.131771
Ratkowsky, D. A., Olley, J., & Ross, T. (2005). Unifying temperature effects on the growth rate of bacteria and the stability of globular proteins. *Journal of Theoretical Biology*, *233*(3), 351–362. https://doi.org/10.1016/j.jtbi.2004.10.016
Reuveni, S., Urbakh, M., & Klafter, J. (2014). Role of substrate unbinding in Michaelis-Menten enzymatic reactions. *Proceedings of the National Academy of Sciences of the United States of America*, *111*(12), 4391–4396. https://doi.org/10.1073/pnas.1318122111
Riley, W. J., Subin, Z. M., Lawrence, D. M., Swenson, S. C., Torn, M. S., Meng, L., et al. (2011). Barriers to predicting changes in global terrestrial methane fluxes: Analyses using CLM4Me, a methane biogeochemistry model integrated in CESM. *Biogeosciences*, *8*(7), 1925–1953. https://doi.org/10.5194/bg-8-1925-2011
Robertson, G. P., & Groffman, P. M. (2015). Nitrogen transformations. In E. A. Paul (Ed.), *Soil microbiology, ecology and biochemistry* (pp. 421–446). Academic Press. https://doi.org/10.1016/b978-0-12-415955-6.00014-1
Salamon, P., Hoffmann, K. H., Schubert, S., Berry, R. S., & Andresen, B. (2001). What conditions make minimum entropy production equivalent to maximum power production? *Journal of Non-Equilibrium Thermodynamics*, *26*(1), 73–83. https://doi.org/10.1515/Jnetdy.2001.006
Salamon, P., Roach, T. N. F., & Rohwer, F. L. (2017). *The ladder theorem*. Paper presented at 14th Joint European Thermodynamics Conference, Budapest, May 21–25.

Sawle, L., & Ghosh, K. (2011). How do thermophilic proteins and proteomes withstand high temperature? *Biophysical Journal*, *101*(1), 217–227. https://doi.org/10.1016/j.bpj.2011.05.059

Schipper, L. A., Hobbs, J. K., Rutledge, S., & Arcus, V. L. (2014). Thermodynamic theory explains the temperature optima of soil microbial processes and high Q(10) values at low temperatures. *Global Change Biology*, *20*(11), 3578–3586. https://doi.org/10.1111/gcb.12596

Schmidt-Rohr, K. (2018). How batteries store and release energy: Explaining basic electrochemistry. *Journal of Chemical Education*, *95*(10), 1801–1810. https://doi.org/10.1021/acs.jchemed.8b00479

Schuster, S., Boley, D., Moller, P., Stark, H., & Kaleta, C. (2015). Mathematical models for explaining the Warburg effect: A review focussed on ATP and biomass production. *Biochemical Society Transactions*, *43*, 1187–1194. https://doi.org/10.1042/BST20150153

Shaver, G. R., & Melillo, J. M. (1984). Nutrient budgets of marsh plants—Efficiency concepts and relation to availability. *Ecology*, *65*(5), 1491–1510. https://doi.org/10.2307/1939129

Shuttleworth, W. J., & Wallace, J. S. (1985). Evaporation from sparse crops—An energy combination theory. *Quarterly Journal of the Royal Meteorological Society*, *111*(469), 839–855. https://doi.org/10.1002/qj.49711146910

Slot, M., & Kitajima, K. (2015). Whole-plant respiration and its temperature sensitivity during progressive carbon starvation. *Functional Plant Biology*, *42*(6), 579–588. https://doi.org/10.1071/FP14329

Smith, O. L. (1976). Nitrogen, phosphorus, and potassium utilization in plant–soil system—Analytical model. *Soil Science Society of America Journal*, *40*(5), 704–714. https://doi.org/10.2136/sssaj1976.03615995004000050029x

Smith, O. L. (1979). Application of a model of the decomposition of soil organic-matter. *Soil Biology and Biochemistry*, *11*(6), 607–618. https://doi.org/10.1016/0038-0717(79)90028-2

Stumm, W., & Morgan, J. J. (1996). *Aquatic chemistry: Chemical equilibria and rates in natural waters*. Wiley.

Swenson, H., & Stadie, N. P. (2019). Langmuir's theory of adsorption: A centennial review. *Langmuir*, *35*(16), 5409–5426. https://doi.org/10.1021/acs.langmuir.9b00154

Taiz, L., & Zeiger, E. (2006). *Plan physiology* (4th ed.). Sinauer Associates, Inc.

Tang, J. Y. (2015). On the relationships between the Michaelis-Menten kinetics, reverse Michaelis–Menten kinetics, equilibrium chemistry approximation kinetics, and quadratic kinetics. *Geoscientific Model Development*, *8*(12), 3823–3835. https://doi.org/10.5194/gmd-8-3823-2015

Tang, J. Y., & Riley, W. J. (2013a). A new top boundary condition for modeling surface diffusive exchange of a generic volatile tracer: Theoretical analysis and application to soil evaporation. *Hydrology and Earth System Sciences*, *17*(2), 873–893. https://doi.org/10.5194/hess-17-873-2013

Tang, J. Y., & Riley, W. J. (2013b). A total quasi-steady-state formulation of substrate uptake kinetics in complex networks and an example application to microbial litter decomposition. *Biogeosciences*, *10*(12), 8329–8351. https://doi.org/10.5194/bg-10-8329-2013

Tang, J. Y., & Riley, W. J. (2017). SUPECA kinetics for scaling redox reactions in networks of mixed substrates and consumers and an example application to aerobic soil respiration. *Geoscientific Model Development*, *10*(9), 3277–3295. https://doi.org/10.5194/gmd-10-3277-2017

Tang, J. Y., & Riley, W. J. (2019a). A theory of effective microbial substrate affinity parameters in variably saturated soils and an example application to aerobic soil heterotrophic respiration. *Journal of Geophysical Research: Biogeosciences*, *124*, 918–940. https://doi.org/10.1029/2018JG004779

Tang, J. Y., & Riley, W. J. (2019b). Competitor and substrate sizes and diffusion together define enzymatic depolymerization and microbial substrate uptake rates. *Soil Biology and Biochemistry*, *139*, 107624. https://doi.org/10.1016/j.soilbio.2019.107624

Tang, J. Y., & Riley, W. J. (2021). Finding Liebig's law of the minimum. *Ecological Applications*.

Thomsen, J. K., Geest, T., & Cox, R. P. (1994). Mass-spectrometric studies of the effect of pH on the accumulation of intermediates in denitrification by *Paracoccus denitrificans*. *Applied and Environmental Microbiology*, *60*(2), 536–541. https://doi.org/10.1128/aem.60.2.536-541.1994

Tilman, D. (1982). *Resource competition and community structure* (1st ed., 296 pp.). Princeton University Press.

Tiwari, J., Fraser, A., & Beckman, R. (1974). Genetic feedback repression. 1. Single locus models, *Journal of Theoretical Biology*, *45*(2), 311–326. https://doi.org/10.1016/0022-5193(74)90117-9

Unden, G., & Bongaerts, J. (1997). Alternative respiratory pathways of *Escherichia coli*: Energetics and transcriptional regulation in response to electron acceptors. *Biochimica et Biophysica Acta: Bioenergetics*, *1320*(3), 217–234. https://doi.org/10.1016/S0005-2728(97)00034-0

Vallis, G. K. (2006). *Atmospheric and oceanic fluid dynamics: Fundamentals and large-scale circulation* (1st ed.). Cambridge University Press.

von Smoluchowski, M. (1917). Versuch einer mathematischen theorie der koagulationkinetik kolloider loesungen. *Zeitschrift für Physikalische Chemie*, *92*, 129–132.

Walker, A. P., Johnson, A. L., Rogers, A., Anderson, J., Bridges, R. A., Fisher, R. A., et al. (2021). Multi-hypothesis comparison of Farquhar and Collatz photosynthesis models reveals the unexpected influence of empirical assumptions at leaf and global scales. *Global Change Biology*, *27*(4), 804–822. https://doi.org/10.1111/gcb.15366

Wu, Y. H., Walker, J., Schwede, D., Peters-Lidard, C., Dennis, R., & Robarge, W. (2009). A new model of bi-directional ammonia exchange between the atmosphere and biosphere: Ammonia stomatal compensation point. *Agricultural and Forest Meteorology*, *149*(2), 263–280. https://doi.org/10.1016/j.agrformet.2008.08.012

Yu, L., Ahrens, B., Wutzler, T., Schrumpf, M., & Zaehle, S. (2020). Jena Soil Model (JSM v1.0; revision 1934): A microbial soil organic carbon model integrated with nitrogen and phosphorus processes. *Geoscientific Model Development*, *13*(2), 783–803. https://doi.org/10.5194/gmd-13-783-2020

Zhang, Z. Y., & Furman, A. (2021). Soil redox dynamics under dynamic hydrologic regimes—A review. *The Science of the Total Environment*, *763*, 143026. https://doi.org/10.1016/j.scitotenv.2020.143026

Zhu, Q., Riley, W. J., & Tang, J. Y. (2017). A new theory of plant–microbe nutrient competition resolves inconsistencies between observations and model predictions. *Ecological Applications*, *27*(3), 875–886. https://doi.org/10.1002/eap.1490